

Microstructure of heteroepitaxial silicon/cobalt disilicide/silicon formed by cobalt implantation into (100) and (111) silicon

Citation for published version (APA):

Bulle-Lieuwma, C. W. T., Ommen, van, A. H., & IJzendoorn, van, L. J. (1989). Microstructure of heteroepitaxial silicon/cobalt disilicide/silicon formed by cobalt implantation into (100) and (111) silicon. *Applied Physics Letters*, 54(3), 244-246. <https://doi.org/10.1063/1.101446>

DOI:

[10.1063/1.101446](https://doi.org/10.1063/1.101446)

Document status and date:

Published: 01/01/1989

Document Version:

Publisher's PDF, also known as Version of Record (includes final page, issue and volume numbers)

Please check the document version of this publication:

- A submitted manuscript is the version of the article upon submission and before peer-review. There can be important differences between the submitted version and the official published version of record. People interested in the research are advised to contact the author for the final version of the publication, or visit the DOI to the publisher's website.
- The final author version and the galley proof are versions of the publication after peer review.
- The final published version features the final layout of the paper including the volume, issue and page numbers.

[Link to publication](#)

General rights

Copyright and moral rights for the publications made accessible in the public portal are retained by the authors and/or other copyright owners and it is a condition of accessing publications that users recognise and abide by the legal requirements associated with these rights.

- Users may download and print one copy of any publication from the public portal for the purpose of private study or research.
- You may not further distribute the material or use it for any profit-making activity or commercial gain
- You may freely distribute the URL identifying the publication in the public portal.

If the publication is distributed under the terms of Article 25fa of the Dutch Copyright Act, indicated by the "Taverne" license above, please follow below link for the End User Agreement:

www.tue.nl/taverne

Take down policy

If you believe that this document breaches copyright please contact us at:

openaccess@tue.nl

providing details and we will investigate your claim.

Microstructure of heteroepitaxial Si/CoSi₂/Si formed by Co implantation into (100) and (111) Si

C. W. T. Bulle-Lieuwma, A. H. van Ommen, and L. J. van IJzendoorn
Philips Research Laboratories, P.O. Box 80 000, 5600 JA Eindhoven, The Netherlands

(Received 20 May 1988; accepted for publication 1 November 1988)

Heteroepitaxial Si/CoSi₂/Si structures have been synthesized by high-dose implantation of Co into (100) and (111) Si at an energy of 170 keV and subsequent annealing. In the as-implanted state the implanted Co is found to be present as CoSi₂. For a dose of 2×10^{17} Co/cm², the Co is present in the form of epitaxial precipitates, which exhibit both the aligned (*A*-type) CoSi₂ and twinned (*B*-type) orientation. For a higher dose of 3×10^{17} Co/cm², a monocrystalline epitaxial CoSi₂ layer near the top of the implanted Co distribution is formed during the implantation. The heteroepitaxial structures that are formed in this way are fully aligned. In contrast, when these structures are formed by sequential surface deposition techniques, twinning occurs at every Si/CoSi₂ interface. The formation of the aligned orientation of the buried CoSi₂ layer can be attributed to the larger stability of aligned precipitates as compared to twin-oriented precipitates.

Heteroepitaxial structures consisting of Si/CoSi₂/Si have received much interest due to their potential application as metal and permeable base transistors.¹ High-dose implantation of Co followed by subsequent annealing is a new and promising technique by which these structures can be formed. White *et al.*² have demonstrated that single crystalline buried CoSi₂ layers can be formed by this technique in both (100) and (111) Si and have named it "mesotaxy." With surface growth methods like evaporation or molecular beam epitaxy (MBE), the formation of monocrystalline CoSi₂ on (100) Si is very difficult due to the competition of different epitaxial orientations with good lattice matching.³ For growth on (111) Si, there is a strong predominance of the twinned (111) *B*-type orientation of CoSi₂ which is rotated through 180° relative to the aligned (111) *A*-type orientation.

We present results on both (100) and (111) Si wafers implanted with 170 keV Co⁺ ions, at an ion current density of $11 \mu\text{A}/\text{cm}^2$, to doses of 2×10^{17} and 3×10^{17} Co⁺/cm². The as-implanted and the annealed wafers were studied. The retained doses were 10% lower, as was evidenced by Rutherford backscattering (RBS). The wafers were externally heated to a temperature of 400 °C, but during the implantation the temperature increased to about 450 °C due to ion beam heating. The substrate temperature was measured by a thermocouple in contact with the wafer. Subsequently, the specimens were annealed for 30 min in a N₂/H₂ ambient at a temperature of 1000 °C. Specimens have been studied in cross section by transmission electron microscopy (Philips EM 400T), high-resolution electron microscopy (Philips EM 430ST), x-ray diffraction (XRD), and Rutherford backscattering spectrometry (using 2 MeV He⁺ ions). A depth resolution of about 10 nm was achieved in the RBS experiments by selecting an angle of 60° between the incident beam and the sample normal.

In all cases, XRD measurements on as-implanted wafers reveal peaks due to CoSi₂ with the same orientation as the Si substrate, as will be discussed in more detail elsewhere.⁴ RBS and transmission electron microscopy (TEM) show that a continuous CoSi₂ layer is formed during the

implantation, only for the highest dose (3×10^{17} Co/cm²).

Figure 1 shows cobalt concentration profiles after implantation of 2×10^{17} Co/cm² in (100) Si and after subsequent annealing. These profiles were determined from the RBS spectra, using a computer program which corrects for composition variations taking into account the dependences of cross sections and stopping powers on the energy of the analyzing He⁺ ions.⁵ In the as-implanted sample, the Co concentration does not reach the level of Co in CoSi₂. This indicates that the concentration of Co is too low to form a continuous CoSi₂ layer. Investigation of the as-implanted structure by cross-sectional TEM reveals that the implanted Co is present in the form of small CoSi₂ precipitates, which are coherent with the Si lattice. In addition to precipitates with the same orientation as the substrate (*A*-type), precipitates which are twin related to the Si matrix (*B*-type) are also observed for both (100) and (111) Si. Figure 2 shows precipitates in implanted (111) Si. It is particularly interesting to note the flat, elongated form of the twinned precipitates, and the fact that they are bounded by {111} planes on the long sides. In some of the twinned precipitates moiré fringes are observed due to overlap with the Si matrix. The

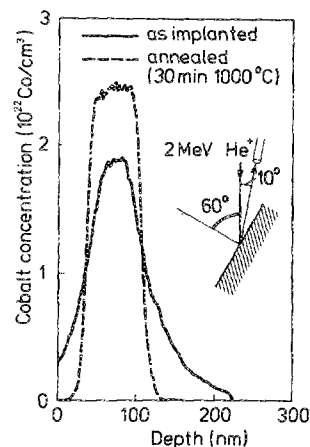


FIG. 1. Cobalt concentration profiles of the as-implanted and annealed sample for (100) Si, as obtained from glancing angle RBS spectra. The implantation dose is 2×10^{17} Co⁺/cm².

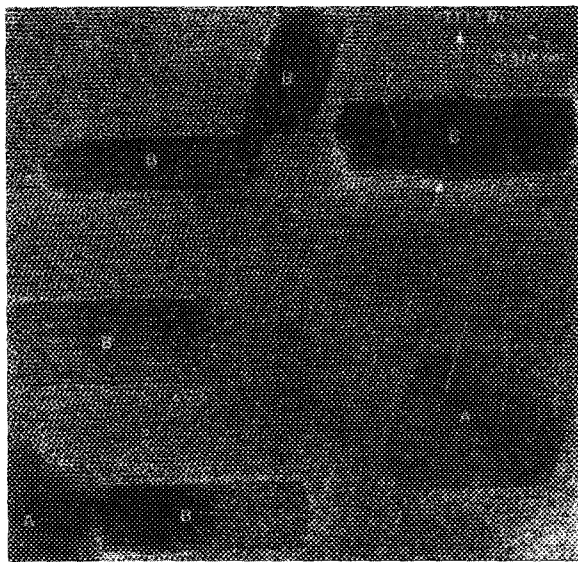


FIG. 2. Cross-sectional HREM image of aligned and twinned CoSi_2 precipitates in as-implanted (111) Si. The implantation dose is $2 \times 10^{17} \text{Co}^+/\text{cm}^2$.

aligned precipitates have a spheroidal shape with occasional $\{100\}$ and $\{111\}$ facets. We observed that for both types of precipitates, their size increases towards the top of the Co concentration profile.

At greater depth, implantation damage is produced in the form of defects on $\{113\}$ Si planes (see Fig. 3). Bourret⁶ has proposed that these defects are formed by precipitation of excess Si interstitials in the form of a hexagonal silicon phase. An excess of interstitials is likely to be present during the implants, and in fact we have found similar defects below buried SiO_2 films synthesized by high-dose implantation of oxygen.⁷

Annealing of the wafer results in the formation of single crystalline buried layers. This is also reflected in the Co concentration profile in Fig. 1, which changes from a Gaussian to a box-shaped distribution with a maximum concentration equal to that of Co in CoSi_2 . Cross-sectional TEM images of buried CoSi_2 layers formed by implantation of $2 \times 10^{17} \text{Co}/\text{cm}^2$ into (100) Si and (111) Si and subsequent annealing are shown in Figs. 4 and 5, respectively. The insets in Figs. 4 and 5 are high-resolution electron microscopy (HREM) images of the CoSi_2/Si interfaces. Annealing has resulted in the formation of a monocrystalline buried CoSi_2 layer, which has sharp interfaces with some small facets. The top and bottom interfaces have the same quality.

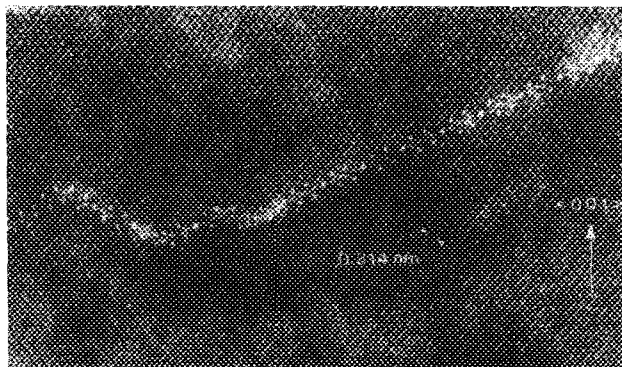


FIG. 3. Cross-sectional HREM image of a $\{113\}$ defect produced by implantation.

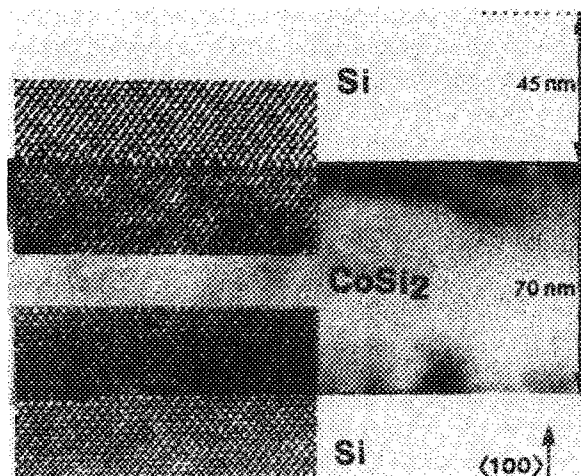


FIG. 4. Cross-sectional TEM micrograph of a buried CoSi_2 layer in (100) Si implanted with $2 \times 10^{17} \text{Co}^+/\text{cm}^2$ and subsequently annealed. The insets are HREM images showing the upper and lower interfaces.

It is important to note that the silicide films are aligned with the substrate, and not twinned as is generally observed when these heterostructures are formed by sequential growth of CoSi_2 and Si.⁸ The formation of a silicide layer with an aligned orientation is the more interesting since Fig. 2 shows that twin-oriented precipitates are present after implantation. Furthermore, when a continuous CoSi_2 layer is formed already during implantation, as is the case with the $3 \times 10^{17} \text{Co}/\text{cm}^2$ implants, these layers are also single crystalline and not twinned. Nevertheless, twin-related precipitates are also observed below these layers. These observations suggest the following explanation of the formation of the aligned structures.

We expect that during implantation both aligned (*A*-type) and twin-oriented (*B*-type) CoSi_2 precipitates are nucleated. It has been argued³ that for surface-grown CoSi_2 on (111) oriented Si, the strain energy caused by the lattice mismatch between CoSi_2 and Si ($\Delta a/a$ is 1.2% at room temperature) possibly leads to the nucleation of twin-oriented CoSi_2 at interfacial steps. Similar arguments are valid for the nucleation of the twinned precipitates during implantation.

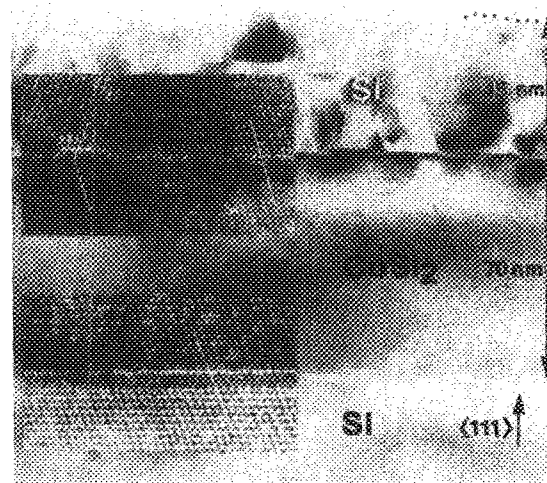


FIG. 5. Cross-sectional TEM image of a buried CoSi_2 layer in (111) Si for an implantation dose of $2 \times 10^{17} \text{Co}^+/\text{cm}^2$. The insets are HREM images of the upper and lower interfaces. Twinning can be seen to have occurred in the top Si film.

Relaxation of misfit strain may also be the driving force for the formation of these precipitates. This is supported by the shape of the twin-oriented precipitates in Fig. 2, in which the long facets represent the $\{111\}$ twin planes. On the other hand, the degree of coherence is much lower for the other facets. It should be noted that this situation is typical for the implanted silicides having a three-dimensional silicide-silicon interface, in contrast to surface-grown silicides where this interface is two dimensional. The aligned precipitates are completely coherent with the Si matrix having $\{100\}$ and $\{111\}$ facets.

During implantation growth and shrinkage of both types of precipitates occur by a process in which larger precipitates grow at the expense of smaller ones. The growth is limited by the diffusion of Co atoms. After implantation we observed at the edges of the Co implantation profile, where the Co concentration is low, precipitates with a minimum size of about 10 nm. After annealing (30 min at 1000 °C) we have found that these precipitates were completely dissolved. This means that there must be a temperature-dependent size below which precipitates are expected to dissolve and precipitates larger than this value are expected to grow.

The most likely explanation for the growth of the aligned structures is the favored growth of *A*-type precipitates. The coherent facets of the *A*-type precipitates allow the precipitate to grow uniformly, resulting in the growth of spheroidal-shaped precipitates. By coalescence of aligned precipitates, aligned precipitates with larger dimensions are formed. For the *B*-type precipitates preferential growth on the disordered facets occurs, resulting in elongated platelet-shaped precipitates (see Fig. 2). There are four sets of twinned precipitates, each set involving another $\{111\}$ twin plane. When precipitates belonging to only *one* single set intersect, they may coalesce and give larger grains. However, when precipitates with different twin planes intersect, the growth of the precipitates is impeded, and during prolonged annealing, dissolution of these precipitates may occur in favor of the continuously growing aligned precipitates. Another possibility is the annihilation of *B* grains by transformation into *A* grains, when an *A*-type precipitate intersects a *B*-type precipitate. Summarizing above-mentioned arguments, aligned precipitates are more stable than the twinned precipitates and will therefore grow at the expense of the twinned ones. Prolonged annealing of the wafers results in the formation of single crystalline layers of aligned orientation.

It is worthwhile to note that for Si wafers implanted with Ni^+ ions we observed no twin-oriented NiSi_2 precipitates in the as-implanted wafers, but only aligned ones. This can be attributed to the much smaller mismatch between NiSi_2 and Si.

TEM analyses of the microstructure after annealing further revealed the presence of threading dislocations ($10^8/\text{cm}^2$) below the silicide layers, whereas misfit dislocations are present at both interfaces. In (100) Si, the top Si film also contains threading dislocations, but it is further monocrys-

talline. For (111) Si, however, the micrographs in Fig. 5 show that the top Si layer is heavily twinned. Probably this phenomenon is responsible for the difference we found⁴ in the RBS channeling yield between the top silicon films of implanted (100) and (111) oriented material. Twin formation is known to occur in (111) Si during elimination of implantation damage.⁹ It is also known that growth of Si on (111) CoSi_2 tends to result in twins which relieve the misfit strain.³ However, it should be noted that White *et al.*,¹⁰ using a lower implantation temperature, have formed buried silicide layers in (111) Si without twinning of the top Si film, indicating that better quality layers can be obtained by optimizing the implantation conditions.

Summarizing, microstructural analyses of Si implanted with a high dose of Co at elevated temperature revealed that the implanted Co is present in the form of CoSi_2 precipitates. These precipitates occur in both aligned and twinned orientations relative to the Si lattice. Implantation of 3×10^{17} Co/cm² results in the formation of a buried epitaxial CoSi_2 layer during the implantation. Annealing of wafers implanted with 2×10^{17} Co/cm² also results in the formation of a Si/ CoSi_2 /Si heteroepitaxial structure. In both cases, the CoSi_2 layer has an aligned orientation relative to the Si lattice. This is unlike what has been observed thus far for CoSi_2 films grown on Si by either reaction of deposited Co or molecular beam epitaxy, where CoSi_2 is predominantly formed in a twinned orientation. The resulting structures exhibit sharp interfaces with some small steps and threading dislocations. At both interfaces, misfit dislocations have been distinguished. It is argued that the preferential growth of aligned precipitates causes the formation of continuous epitaxial layers with an aligned orientation. Concluding, this microstructural study has clearly demonstrated the occurrence of some unique phenomena during synthesis of heteroepitaxial Si/ CoSi_2 /Si structures by high-dose implantation of Co into Si.

¹J. C. Hensel, A. F. J. Levi, R. T. Tung, and J. M. Gibson, *Appl. Phys. Lett.* **47**, 151 (1985).

²A. E. White, K. T. Short, R. C. Dynes, J. P. Garno, and J. M. Gibson, *Appl. Phys. Lett.* **50**, 95 (1987).

³C. W. T. Bulle-Lieuwma, A. H. van Ommen, and J. Hornstra, *Mater. Res. Soc. Symp. Proc.* **102**, 377 (1988).

⁴A. H. van Ommen, J. J. M. Ottenheim, A. M. L. Theunissen, and A. G. Mouwen, *Appl. Phys. Lett.* **53**, 669 (1988).

⁵P. Borgesen, R. Behrish, and B. M. U. Scherzer, *Appl. Phys. A* **27**, 183 (1982).

⁶A. Bourret, *Proceedings of Microscopy of Semiconducting Materials Conference* (Institute of Physics, Bristol, 1987), Institute of Physics Conference Series No. 87, p. 39.

⁷A. H. van Ommen, B. H. Koek, and M. P. A. Vieggers, *Appl. Phys. Lett.* **49**, 628 (1986).

⁸R. T. Tung, J. M. Poate, J. C. Bean, J. M. Gibson, and D. C. Jacobson, *Thin Solid Films* **93**, 77 (1982).

⁹G. Foti, L. Csepregi, E. F. Kennedy, and J. W. Mayer, *Philos. Mag. A* **37**, 591 (1978); M. D. Rechting and P. P. Pronko, *ibid.* **37**, 605 (1978).

¹⁰A. E. White, K. T. Short, R. C. Dynes, J. P. Garno, and J. M. Gibson, *Mater. Res. Soc. Symp. Proc.* **74**, 481 (1987).